

1 **Structural characterization of the jasmonoyl-isoleucine**  
2 **perception complexes from *Fragaria vesca* by in silico**  
3 **molecular analysis**

4  
5 Felipe Valenzuela-Riffo<sup>1+</sup>, Adrián Garrido-Bigotes<sup>2,3+</sup>, Pablo M. Figueroa<sup>3\*</sup>, Luis Morales-Quintana<sup>1\*</sup>,  
6 Carlos R. Figueroa<sup>3\*</sup>

7  
8 <sup>1</sup>Institute of Biological Sciences, University of Talca, Talca, Chile.

9 <sup>2</sup>Doctorate Program in Forest Sciences, University of Concepción, Concepción, Chile

10 <sup>3</sup>Phytohormone Research Laboratory, Institute of Biological Sciences, University of Talca, Talca, Chile.

11

12 <sup>+</sup> These authors contributed equally to this work.

13

14 \* Corresponding authors:

15 Pablo M. Figueroa

16 Phytohormone Research Laboratory, Institute of Biological Sciences, University of Talca, Talca, Chile.

17 E-mail address: pabfigueroa@utalca.cl

18

19 Luis Morales-Quintana

20 Institute of Biological Sciences, University of Talca, Talca, Chile.

21 E-mail address: lmorales@utalca.cl

22

23 Carlos R. Figueroa

24 Phytohormone Research Laboratory, Institute of Biological Sciences, University of Talca, Talca, Chile.

25 E-mail address: cfigueroa@utalca.cl

26

27 **Abstract**

28

29 **Background.** The phytohormone jasmonates (JAs) regulate fundamental plant processes; such  
30 as the anthocyanin accumulation during ripening of strawberry, a non-climacteric fruit model.  
31 Jasmonoyl-isoleucine (JA-Ile), one of the bioactive JA molecules, mediates binding of the JAZ  
32 repressor protein to COI1, an F-box protein forming the SCF<sup>COI1</sup> ubiquitin E3 ligase complex, in  
33 Arabidopsis. The COI1-JA-Ile-JAZ complex initiates the JA-signaling pathway leading to early  
34 jasmonate responses. Most of Arabidopsis JAZs contain a degron sequence at the Jas domain  
35 responsible for interaction with COI1 and JA-Ile. The woodland strawberry (*Fragaria vesca*) is a  
36 model plant for the Rosaceae family, in which the JA-signaling pathway is poorly understood at  
37 the molecular level. The aim of this work was to understand the molecular basis of the  
38 interaction between the *F. vesca* COI1 (FvCOI1) and JAZ1 (FvJAZ1) or JAZ8 (FvJAZ8)  
39 mediated by JA-Ile.

40 **Methods.** Multiple alignments of amino acid sequences and phylogenetic analyses were  
41 performed for FvCOI1 and FvJAZ1/8 and their ortholog sequences. The FvCOI1 and FvJAZ1/8  
42 3D structures were built by homology modeling methods, which were further refined and  
43 validated by molecular dynamics simulation (MDS). A molecular docking approach along with  
44 MDS analysis were used to understand the interaction capacity between a putative degron-like  
45 present in FvJAZ1 and FvJAZ8 with the FvCOI1-JA-Ile and FvCOI1-JA complexes.

46 **Results.** FvCOI1 and FvJAZ1/8 showed high and moderate identity, respectively, with the  
47 corresponding ortholog proteins from other plant species including apple, grape, tomato and  
48 Arabidopsis. The resulting FvCOI1 structural model showed that the F-box and LRR domains  
49 were highly similar to that described in Arabidopsis COI1 (AtCOI1) crystal structure.  
50 Unexpectedly, we found that FvJAZ1 has a variant IPMQRK sequence respect to the canonical  
51 LPIAR(R/K) degron sequence observed in AtJAZ1. The MDS results showed that the FvCOI1-  
52 JA-Ile-FvJAZ1 complex was the most stable among all the analyzed ones, and the IPMQRK  
53 peptide of FvJAZ1 interacted directly with FvCOI1 and JA-Ile. In contrast, FvJAZ8 did not show  
54 a direct interaction with those two components, as expected from previous experimental results  
55 for the ortholog AtJAZ8.

56 **Discussion.** The present research provides novel insight into the molecular interactions between  
57 key JA-signaling components in the model plant *F. vesca*. Remarkably, we characterized the

58 IPMQRK sequence present in FvJAZ1, a putative variant of the canonical degron previously  
59 described in AtJAZ1. We propose that the FvCOI1-JA-Ile-FvJAZ1 complex is stable, and that  
60 the degron-like sequence present in FvJAZ1 interacts in a steady manner with FvCOI1-JA-Ile.  
61 Up to now, this is the first structural characterization of molecular interactions that may be  
62 occurring between the core components of the JA-Ile perception complex in a fleshy fruit-related  
63 species.

## 64 Introduction

65  
66 Jasmonates (JAs) are phytohormones that regulate environmental adaptation and development in  
67 plants (Chini et al., 2016). Recently, it has been shown that JAs regulate early development and  
68 anthocyanin accumulation in grape and strawberry fruits, respectively (Concha et al., 2013;  
69 Böttcher et al., 2015) pointing out a role in development and ripening of non-climacteric fruits.  
70 Physiological effects of JAs are mediated by the bioactive molecule, (+)-7-*iso*-jasmonoyl-L-  
71 isoleucine (JA-Ile) in Arabidopsis (Fonseca et al., 2009), which is structurally and functionally  
72 analogous to the bacterial phytotoxin coronatine (COR, Katsir et al., 2008). However, recently  
73 others bioactive (+)-7-*iso*-amino acid conjugates have been reported in Arabidopsis and other  
74 plants (Yan et al., 2016).

75  
76 JA-Ile performs its physiological effects by activating the JA-signaling pathway, and this is now  
77 beginning to be well understood in Arabidopsis (Pérez & Goossens, 2013). The F-box  
78 CORONATINE INSENTIVE 1 (COI1) protein is part of the SKP1/CUL1/F-box (SCF<sup>COI1</sup>)  
79 ubiquitin E3 ligase complex (Xu et al., 2002). The *coi1* null mutant has impaired JA responses in  
80 Arabidopsis (Xie et al., 1998). COI1 binds to JASMONATE ZIM-DOMAIN (JAZ) repressor  
81 protein when JA-Ile accumulates (Chini et al., 2007; Thines et al., 2007; Yan et al., 2007) to  
82 conform the COI1-JAZ co-receptor (Sheard et al., 2010). Then, the JAZ protein is degraded by  
83 the 26S proteasome after ubiquitination (Chini et al., 2007; Thines et al., 2007) and now, MYC  
84 transcription factors (Lorenzo et al., 2004; Fernández-Calvo et al., 2011; Niu, Figueroa &  
85 Browse, 2011; Figueroa & Browse, 2015) induce the expression of early-JA response genes  
86 (Chini et al., 2007). In the absence of JA-Ile, JAZ binds to MYCs repressing the expression of  
87 early JA response genes (Chini et al., 2007; Thines et al., 2007; Chung et al., 2008). These core  
88 components establish the initiation of the JA signaling pathway to regulate JA responses in  
89 terrestrial plants (Chini et al., 2016).

90  
91 Arabidopsis COI1 (AtCOI1) amino acid sequence contains leucine-rich repeats (LRRs) and F-  
92 box domains, similar to the auxin receptor TRANSPORT INHIBITOR RESPONSE1 (TIR1)  
93 (Tan et al., 2007; Yan et al., 2009). JAZ belongs to the TIFY family with 12 members in  
94 Arabidopsis (Chini et al., 2007). These proteins contain the TIFY domain for binding themselves

95 or to other JAZ and Novel Interactor of JAZ (NINJA) adaptor protein (Vanholme et al., 2007;  
96 Pauwels et al., 2010). Moreover, Arabidopsis JAZs (AtJAZs) contains a Jas domain (a CCT  
97 domain) that interacts with COI1 and transcription factors for its degradation and repression of  
98 early-JA responses, respectively (Chini et al., 2007, Katsir et al., 2008, Melotto et al., 2008).  
99 Most of AtJAZs contain the canonical LPIAR(R/K) degron sequence at the Jas domain that is  
100 responsible for interaction with COI1 and JA-Ile (Sheard et al., 2010). However, AtJAZ8 lacks  
101 this canonical degron sequence and its transcriptional repression activity is mediated by a N-  
102 terminal EAR motif allowing recruitment of TOPLESS co-repressors to repress the JA-signaling  
103 pathway by a NINJA-independent molecular mechanism in Arabidopsis (Shyu et al., 2012).

104  
105 AtCOI1 interacts with JAZ in the presence of JA-Ile and its mimic COR molecule (Katsir et al.,  
106 2008). Its 3D structure was reported firstly using a molecular modeling approach (Yan et al.,  
107 2009) and then by a crystallographic study (Sheard et al., 2010). AtCOI1 consists of a packed  
108 structure composed by  $\alpha$ -helix and  $\beta$ -sheets forming LRR domains, which are required for  
109 protein stability (Yan et al., 2009; Sheard et al., 2010). On the other hand, AtCOI1 contains a  
110 surface pocket with amino acid residues necessary for binding to JAZ in the presence of JA-Ile  
111 (Yan et al., 2009; Sheard et al., 2010). Recently, Sen et al. (2016) proposed the COI1 structural  
112 models for five monocot species (rice, wheat, maize, *Sorghum* and *Setaria*), and evaluated their  
113 interaction with JA-Ile and the JAZ1 degron sequence from the herbaceous plant finger millet.  
114 The authors showed that the five models were highly similar at structural level, indicating a  
115 highly conserved structure for COI1 in monocots (Sen et al., 2016). Experimental and in silico  
116 studies showed that the most likely interaction model among the COI1, JAZ and JA-Ile  
117 molecules consists in COI1 binding first to JA-Ile and then both to JAZ (Yan et al., 2009).  
118 However, a protein crystallographic study and additional experimental results reveal a different  
119 interaction model, in which COI1-JAZ acts as a co-receptor complex for perception of JA-Ile in  
120 Arabidopsis (Sheard et al., 2010). In this interaction model, COI1 LRR domains form a TIR1-  
121 like structure with a surface pocket for JA-Ile binding (Yan et al., 2009; Sheard et al., 2010). On  
122 the other hand, JAZ1 canonical LPIAR(R/K) degron sequence acts like a clamp closing the  
123 binding pocket to wraps JA-Ile (Sheard et al., 2010). Moreover, inositol pentakisphosphate  
124 (InsP5) is a COI1 cofactor that increases the perception sensitivity to JA-Ile in Arabidopsis  
125 (Sheard et al., 2010).

126  
127 Until now, the molecular mechanisms underlying the JA-Ile perception and early responses are  
128 not well known in any other plant except Arabidopsis and at a lower extend in a heterologous co-  
129 receptor formed by finger millet JAZ1 and COI1 from several monocots. The aim of this  
130 research is to characterize the interaction between the *Fragaria vesca* COI1 (FvCOI1) and  
131 JAZ1/8 (FvJAZ1/8) mediated by JA-Ile to form the hormone-bound co-receptors to reveal the  
132 molecular mechanism involved in JA-Ile perception in a model organism for studies in *Fragaria*  
133 genus and climacteric fruits.

134

## 135 **Materials and methods**

136

### 137 **Sequences analysis**

138

139 The full-length inferred amino acid sequences of FvCOI1, FvJAZ1, and FvJAZ8 were obtained  
140 from *F. vesca* genome database version 2.0 ([www.rosaceae.org](http://www.rosaceae.org); January 23, 2017) using the  
141 Arabidopsis AtCOI1, AtJAZ1 and AtJAZ8 sequences as queries. For FvCOI1, a single sequence  
142 (accession code: XP\_004307613) with a high identity (69.8%) relative to AtCOI1 was found. In  
143 the case of FvJAZ1 and FvJAZ8, we selected the sequences that showed the highest identity  
144 respect to Arabidopsis orthologs. The amino acid sequences of FvJAZ1 (accession code:  
145 XP\_004287655) and FvJAZ8 (accession code: XP\_004293626) that exhibited 38.7% and 46.2%  
146 of sequence identity relative to AtJAZ1 and AtJAZ8, respectively, were selected for further  
147 studies (Table S1). Thus, in the present research, the XP\_004307613, XP\_004287655,  
148 XP\_004293626 sequences were named as FvCOI1, FvJAZ1 and FvJAZ8, respectively. A search  
149 on the RCSB Protein Data Bank (January 3, 2017) confirmed that X-ray crystal structure for  
150 FvCOI1, FvJAZ1 and FvJAZ8 proteins were not publically available. A multiple alignment of  
151 amino acid sequences was performed using Clustal W and Bioedit Sequence Alignment Editor  
152 v7.0 software (Hall, 1999). Phylogenetic analyses were conducted using MEGA v7.0 software  
153 (Kumar, Stecher & Tamura, 2016), using the Neighbor-Joining methodology and a bootstrap  
154 analysis of 1000 replicates. The following GenBank accession numbers corresponding to the  
155 full-length amino acid sequences were used: FvCOI1 (*F. vesca* COI1, XP\_004307613), FvJAZ1  
156 (*F. vesca* JAZ1, XP\_004287655), FvJAZ8 (*F. vesca* JAZ8, XP\_004293626), AtCOI1

157 (*Arabidopsis thaliana* COI1, NP\_565919), AtJAZ1 (*A. thaliana* JAZ1, NP\_564075), AtJAZ8 (*A.*  
158 *thaliana* JAZ8, NP\_564349), VvCOI1 (*Vitis vinifera* COI1, AFF57759), VvJAZ9 (*V. vinifera*  
159 JAZ9, XP\_002277157), VvJAZ3 (*V. vinifera* JAZ3, XP\_003634826), SlCOI1 (*Solanum*  
160 *lycopersicum* COI1, NP\_001234464), SlJAZ1 (*S. lycopersicum* JAZ1, XP\_004243696), SlJAZ8  
161 (*S. lycopersicum* JAZ8, XP\_004244919), MdCOI1 (*Malus ×domestica* COI1, XP\_008392915),  
162 MdJAZ1 (*M. ×domestica* JAZ1, XP\_008388962), MdJAZ3 (*M. ×domestica* JAZ3,  
163 XP\_008371611) and MdJAZ4 (*M. ×domestica* JAZ4, XP\_008371611).

164

### 165 **Building the protein structure using comparative modeling**

166

167 The protein model for FvCOI1, FvJAZ1, and FvJAZ8 were built according to the method  
168 described by Morales-Quintana et al. (2011), using MODELLER 9v17 software  
169 (<http://salilab.org/modeller/>) by a comparative modeling methodology. The crystal structure  
170 (PDB code 3OGK) for Arabidopsis complex, which corresponds to COI1 protein co-crystalized  
171 with JAZ1 degron was selected as template for further studies. A SPC pre-equilibrated water  
172 model was used for each protein model, and then the system was neutralized by adding NaCl.  
173 After that, the system was equilibrated by molecular dynamics simulations (MDS) during 10 ns  
174 of using SCHRÖDINGER suite with OPLS v2005 force field (Jorgensen, Maxwell & Tirado-  
175 Rives, 1996). The protein protonation state was set to pH 7.2 since this value was reported in  
176 plant cell nucleus (Shen et al., 2013). To evaluate the model both PROCHECK (Laskowski et al.,  
177 1993) and ProSA2003 (Sippl, 1993) programs were employed.

178

### 179 **Protein-ligand interactions**

180

181 At first, a molecular docking method was used to predict the putative binding interaction modes.  
182 For this purpose, two different docking analyses were carried out. The first one used JA-Ile or  
183 jasmonic acid (JA) molecules (as a negative control) for binding to FvCOI1 using the AutoDock  
184 vina program (Trott & Olson, 2010); the last docking run was performed with FvJAZ1 or  
185 FvJAZ8 bound to FvCOI1-JA and FvCOI1-JA-Ile complexes separately using HADDOCK  
186 (Dominguez, Boelens & Bonvin, 2003; de Vries et al., 2007). The assembly order for the  
187 FvCOI1-JA-Ile-FvJAZ1, FvCOI1-JA-Ile-FvJAZ8, FvCOI1-JA-FvJAZ1, and FvCOI1-JA-



188 FvJAZ8 complexes was performed according to Yan et al. (2009). Five independent docking  
189 runs were carried out, and 10 conformers were obtained in each case.

190  
191 Then, MDS for each complex was studied. The initial coordinates for simulations were taken  
192 from the docking experiments described above. Each complex was embedded into a SPC pre-  
193 equilibrated water model and then neutralized by adding NaCl to the system. Each MD  
194 simulation was performed at constant pressure (1.01325 bar) and temperature (300 K) values,  
195 with a NVT ensemble. During 100 ns of each MDS, only the secondary structure for FvCOI1  
196 had a  $0.25 \text{ kcal mol}^{-1} \text{ \AA}^{-2}$  spring constant. Data were collected every 50 ps trajectory. Finally, all  
197 MDS were analyzed using the VMD software (Humphrey, Dalke & Schulten, 1996).

198

## 199 **Results**

200

### 201 **FvCOI1 and FvJAZ1/8 sequence analysis**

202

203 We compared COI1, JAZ1 and JAZ8 amino acid sequences among *Fragaria vesca* and three  
204 fleshy fruit-related species, aside from Arabidopsis. We analyzed sequences from *V. vinifera* and  
205 *S. lycopersicum* because their importance as models for non-climacteric and climacteric fruit  
206 ripening, respectively, and from *M. ×domestica* as representative species belonging to the  
207 Rosaceae family as *F. vesca*.

208

209 Multiple sequence alignments were performed to estimate the identity between FvCOI1 protein  
210 and its orthologs from the plant species described above. Then, a phylogenetic tree was  
211 constructed to reveal evolutionary relationships between these proteins. FvCOI1 sequence was  
212 highly conserved respect to AtCOI1, VvCOI1, SlCOI1 and MdCOI1 (Fig. 1A) displaying  
213 identity values higher than 69.8% (Table S2). Specifically, FvCOI1 exhibited the highest  
214 sequence identity with MdCOI1 (82.3%) (Table S2). FvCOI1 showed an F-box domain, 18 LRR  
215 domains and specific amino acid residues for binding to JA-Ile (R81, R345, Y383, R406, and  
216 R493), which are highly conserved between the analyzed COI1 orthologs (Fig. 1A).  
217 Phylogenetic analysis showed a close relationship between FvCOI1 and MdCOI1 or VvCOI1



218 rather than SlCOI1 or AtCOI1 (Fig. 1B). These results indicate that FvCOI1, MdCOI1 and  
219 VvCOI1 diverged more recently from a common ancestor.

220  
221 TIFY protein family includes JAZ proteins (Vanholme et al., 2007). The predicted TIFY protein  
222 sequences, TIFY10A and TIFY5A were found in *F. vesca* protein database and named as  
223 FvJAZ1 and FvJAZ8 respectively, according to their identities (Table S1). A multiple sequence  
224 alignment and phylogenetic analysis for JAZ1/8 ortholog proteins were performed to estimate  
225 the similarity degree and evolutionary relationships between them. We found that MdJAZ1,  
226 SlJAZ1 and VvJAZ9 were the orthologs for FvJAZ1 along with AtJAZ1 based on sequence  
227 identity (Table S2). FvJAZ1 showed higher sequence identity with MdJAZ1 (57.6%) (Table S2).  
228 On the other hand, FvJAZ8 showed higher sequence identity with VvJAZ3 (61.1%), MdJAZ3  
229 (65.5%) and MdJAZ4 (65.5%) (Table S2). All analyzed JAZ sequences showed TIFY and Jas  
230 domains (Fig. 2B, C), while the canonical LPIAR(R/K) degron sequence was absent in all JAZ8  
231 orthologs (Fig. 2C). Remarkably, FvJAZ1 contained an IPMQRK sequence instead of  
232 LPIAR(R/K) degron differing from the other ortholog sequences that contain the canonical  
233 LPIAR(R/K) sequence (Fig. 2C). The Jas domain central (SLX<sub>2</sub>FX<sub>2</sub>KRX<sub>2</sub>R) and C-terminal  
234 (X<sub>5</sub>PY) regions were highly conserved among all FvJAZ1/8 orthologs (Fig. 2C). In addition, a  
235 protein sequence alignment showed the absence of the LPIAR(R/K) sequence in FvJAZ8 and the  
236 respective orthologs, as expected in AtJAZ8 (Shyu et al., 2012) (Fig. 2C). AtJAZ8 presented the  
237 X<sub>3</sub>SMK motif instead of the canonical degron sequence (Shyu et al., 2012). In our work, we  
238 found a conserved SMK sequence in all FvJAZ8 orthologs with the exception of SlJAZ10, which  
239 presented a TVK variant sequence (Fig. 2C). In turn, the EAR motif (LxLxL; Shyu et al., 2012)  
240 was present in all FvJAZ8 orthologs analyzed, with the exception of VvJAZ3 (Fig. 2A). Finally,  
241 a phylogenetic analysis grouped FvJAZ1/8 and ortholog proteins in groups II and I, respectively  
242 (Fig. 2D), exhibiting FvJAZ1 and FvJAZ8 an even more close evolutionary relationship with  
243 MdJAZ1 and AtJAZ8, respectively (Fig. 2D). Additionally, we analyzed 37 inferred JAZ  
244 sequences from different plant species (Fig. S1). We observed that the canonical [LPIAR(R/K)]  
245 degron sequence was present in 24 sequences while in the remaining 13 sequences it was less  
246 conserved, including the IPMQRK sequence found in FvJAZ1.

247

248 Globally, these results show that domains, motifs and amino acids residues, which participate in  
249 Arabidopsis COI1-JAZ interaction dependent on JA-Ile, are highly conserved in *F. vesca* and  
250 other orthologs, with the exception of the putative IPMQRK degron sequence that we observed  
251 in FvJAZ1.

252

### 253 **3D structure of FvCOI1 based on comparative modeling**

254

255 COI1 is a central component of the core module involved in jasmonate signaling and response.  
256 Until now, a 3D structure for FvCOI1 is not known. We used various in silico tools to obtain  
257 insights into the molecular mechanism that is responsible of FvCOI1 interaction with JA-Ile and  
258 FvJAZs. A 3D model for FvCOI1 was built based on sequence alignment between FvCOI1 and  
259 AtCOI1 template (69.8% identity). Two further optimization steps were performed to obtain a  
260 correct model for FvCOI1. First, an energy minimization procedure was performed, and after  
261 that, a short molecular dynamics simulation was run to achieve a final structural model for  
262 FvCOI1 (Fig. 3). A geometric and energetic model evaluation was performed to validate its  
263 quality. The RMSD values calculated between FvCOI1 and its template for the backbone was  
264 10.8 Å (Fig. S2). The stereochemical quality of the 3D model was analyzed using Ramachandran  
265 plots generated by PROCHECK. It was found that the  $\phi/\psi$  angles for most of the amino acid  
266 residues were at the favored region of 99.4% (including: most favorable regions, additional  
267 allowed regions and generously allowed regions) indicating a good stereochemical quality (Table  
268 S3). Finally, the FvCOI1 model showed a Z-score of -9.07 according to ProSA2003, which was  
269 close to -8.13 value obtained for the Arabidopsis template. Consequently, the final structure for  
270 FvCOI1 was acceptable for further analysis.

271

272 Regarding to the properties for the FvCOI1 structural model, it was formed by two domains,  
273 which revealed a TIR1-like overall architecture (Tan et al., 2007): a small N-terminal tri-helical  
274 F-box domain and a large LRR domain (Fig. 3A). The LRR domain included seventeen LRR  
275 domains, which adopted a tandem packed structure of staggered  $\alpha$ -helix and  $\beta$ -sheets (Fig. 3B).  
276 FvCOI1 had a central cavity in the LRR domain; the top of the cavity surface was formed by  
277 three long loops (Fig. 3B), similar to AtTIR1 and AtCOI1 (Tan et al., 2007). This cavity is  
278 involved in hormone binding and to recognize the JAZ polypeptide substrate (Sheard et al.,

279 2010).

280

### 281 **3D structure for FvJAZ1/8 based on comparative modeling studies**

282

283 JAZs are key components of the JA-Ile co-receptor by forming a hormone-dependent complex  
284 with COI1. To understand how this interaction works at molecular level, it was necessary to  
285 obtain the FvJAZ 3D structures. A search on the RCSB Protein Data Bank confirmed that was  
286 not publically available any X-ray crystal structure for any JAZ proteins, and only exists the  
287 AtJAZ1 Jas domain (including the degron peptide) co-crystalized with AtCOI1 (Sheard et al.,  
288 2010). Consequently, it was only possible to model the Jas domain of the FvJAZ1 and FvJAZ8  
289 proteins. For this, a sequence alignment between the AtJAZ1 template fragment and our  
290 sequences was performed. Then, the non-aligned sequence was removed and only the sequence  
291 similar to the template fragment was considered for each FvJAZ (Fig. S3A). Similar to FvCOI1  
292 model described above, two optimization steps were performed to obtain a correct model,  
293 followed by an energetic and geometric evaluation. The RMSD values for the backbone and  
294 calculated between AtJAZ1 and the two FvJAZ structures were 3.79 Å (Fig. S3D). Additionally,  
295 the RMSD value calculated between FvJAZ1 and FvJAZ8 was 2.9 Å (Fig. S3E). The  
296 PROCHECK showed that all amino acid residues were at the favored region respect to FvJAZ1  
297 and FvJAZ8 (Table S3). Finally, the Z-score for FvJAZ1 and FvJAZ8 was -2.34 and -1.75  
298 respectively, while the template showed a Z-score of -1.29. The final structures for FvJAZ1 and  
299 FvJAZ8 peptides were acceptable for further analysis.

300

301 Regarding to the structural characteristics of the FvJAZ1 and FvJAZ8 peptide fragments (Fig.  
302 S3B, C, respectively), they adopted a bipartite structure with a loop region followed by a small  
303  $\alpha$ -helix for assembling with the COI1–JA-Ile complex (Sheard et al., 2010).

304

### 305 **FvCOI1-ligand interaction**

306

307 To elucidate whether FvCOI1 binds directly to JA-Ile or JA (used as a negative control), we  
308 evaluated FvCOI1–JA-Ile/JA interactions by molecular docking methodology to generate each  
309 corresponding protein-ligand complex. As shown in Table 1, a negative energy was obtained for

310 each tested ligand, indicating a favorable or likely protein-ligand interaction. However, the  
311 differences between ligands were significant, being the strongest binding interaction found  
312 between JA-Ile and FvCOI1 (Table 1).

313  
314 To corroborate that FvCOI1 has a stronger interaction with JA-Ile than JA as we expected, MDS  
315 studies were performed. The time-course FvCOI1-ligand interaction for JA-Ile and JA was  
316 studied using MDS. The complex formed between FvCOI1 and JA-Ile showed a correct  
317 orientation as the previously described template structure for AtCOI1-JA-Ile complex. JA-Ile  
318 was oriented in the pocket entrance of FvCOI1, and sat in an ‘upright’ position with the keto  
319 group of its common cyclopentanone ring pointing up and forming a hydrogen bond (H-bond)  
320 with R493 and K8 residues from FvCOI1 (Fig. 4A). Additionally, other amino acid residues  
321 were important for the protein-ligand interaction, contributing to the FvCOI1 pocket entrance  
322 architecture (Fig. 4A). In contrast, the ligand in FvCOI1-JA complex (Fig. 4B) was incorrectly  
323 oriented in relation to the JA-Ile previously described by Sheard et al. (2010) and shown in Fig  
324 4A, where its orientation was perpendicular with respect to JA-Ile, and located more distant to  
325 the K8 residue, forming a H-bond only with Y441.

326

### 327 **FvJAZ1/8 binding to FvCOI1-JA-Ile and FvCOI1-JA**

328

329 The previously generated FvCOI1-JA-Ile and FvCOI1-JA stable complexes were used to study  
330 protein-ligand-protein conformations by molecular docking simulation procedure using the  
331 FvJAZ1 and FvJAZ8 peptide fragments. As shown in Table 2, negative values of Haddock score  
332 were obtained for the four tested complexes, indicating a favorable or likely protein-ligand-  
333 protein interaction. The strongest binding interaction was found between FvJAZ1 and FvCOI1  
334 with JA-Ile (Table 2), however, the two complexes with FvJAZ8 showed an unfavorable  
335 Haddock score.

336

337 The different formed complexes were evaluated by MDS procedure. First, the dependence on  
338 RMSD values was tested to check whether the convergence in calculations was obtained and if  
339 the equilibrated MD trajectory was stable. The RMSD value for FvCOI1-JA-Ile-FvJAZ1  
340 complex was the lowest one, with a value around 0.9 Å (Fig. S4) indicating a conformational

341 high stability for the protein structures. In the other three complexes the stability value was  
342 obtained only at the final part of the MD trajectory, observing higher RMSD values (around 1.5  
343 and 2.0 Å) of RMSD respect to FvCOI1-JA-Ile-FvJAZ1 complex (Fig. S4).

344  
345 Regarding to the orientation of the structures in the different complexes, the short structure for  
346 FvJAZ1 and FvJAZ8 was situated on top of the hormone-binding pocket (Fig. 5 and 6,  
347 respectively). Although, FvJAZ1 simultaneously interacted with both FvCOI1 and the ligand  
348 (JA-Ile or JA), its pocket only coordinated in a stable manner with JA-Ile (Video S1). This due to  
349 the fact that JA is more mobile and it started to separate from the complex (Fig. 5D, E; Video  
350 S2). In contrast, the two complexes with FvJAZ8 showed a stable coordination with the ligands  
351 (JA-Ile and JA) in the pocket. However, FvJAZ8 was more mobile during the MDS and it  
352 separated from the complexes formed by FvCOI1 and both jasmonate molecules (Fig. 6A, B, D,  
353 E; Video S3, S4).

354  
355 During the MDS of FvCOI1-JA-Ile with FvJAZ1 different H-bonds were formed between amino  
356 acid residues of each protein and JA-Ile. As shown in the Figure 5C, the K8, K79, S145, and  
357 Y441 residues formed an H-bond with frequency values of 70%, 36%, 55%, and 67%,  
358 respectively. As described before, JA distanced itself from the FvCOI1-FvJAZ1 complex during  
359 the MDS (with a distance over 4 Å), explained the observed lower frequency value compared to  
360 JA-Ile as ligand. Using a 30% of frequency values as threshold, only Y441 residue form an H-  
361 bond with JA with 67% of frequency value (Fig. 5F up). Additionally, the total number of H-  
362 bonds was highest in the complex containing JA-Ile instead of JA, with an average of 3 or 4 H-  
363 bonds, while in the complex with JA and FvJAZ1 it contained 1 or 2 H-bonds (Fig. 5C down and  
364 5F down). In the complexes formed between FvCOI1-JA-Ile or FvCOI1-JA with FvJAZ8 there  
365 was a long separation (more than 6-8 Å) between FvJAZ8 and the complex during a longer time  
366 of the MDS, and the H-bond formation was lower with one or two amino acid residues forming  
367 H-bonds (Fig. 6C up and 6F up). Finally, the total number of H-bonds formed between the  
368 different components of the FvCOI1-JA-Ile-FvJAZ8 complex was lower than the FvCOI1-JA-  
369 Ile-FvJAZ1 complex, which presented on average 1 or 2 H-bonds (Fig. 6C down and 6F down).

370

## 371 Discussion

372

373 **Identification and characterization of FvCOI1 and FvJAZ1/8 amino acid sequences**

374

375 The perception of JA-Ile is critical for initiation of JA signaling pathway (Sheard et al., 2010).  
376 COI1 is a highly conserved F-box protein in terrestrial plants, part of the SKP1/CUL1/F-box  
377 (SCF<sup>COI1</sup>) ubiquitin E3 ligase complex, that together with JAZs acts as a JA-Ile co-receptor (Han,  
378 2016). The F-box and LRR domains present in AtCOI1 are critical for protein stabilization and  
379 JAZ interaction, respectively (Sheard et al., 2010), and were highly conserved in FvCOI1 (Fig.  
380 1A). On the other hand, R85, R348, Y386, R409 and R496 residues, which participate in binding  
381 to JA-Ile in Arabidopsis (Sheard et al., 2010), were also conserved in FvCOI1 (represented by  
382 R81, R345, Y383, R406 and R493) and ortholog proteins such as VvCOI1, SlCOI1 and MdCOI1  
383 (Fig. 1A). The observed high conservation on F-box and LRR domains, presence of key amino  
384 acid residues for JA-Ile binding, and evolutionary relationships between COI1 orthologs suggest  
385 that FvCOI1 is a functional protein involved in the JA signaling pathway in strawberry.

386

387 On the other hand, JAZ are repressors of the JA-signaling pathway (Chini et al., 2007; Thines et  
388 al., 2007; Yan et al., 2007). In *A. thaliana* and *S. lycopersicum* 12 JAZ proteins have been  
389 described, whereas in *M. ×domestica* and *V. vinifera* the number is 18 and 11, respectively  
390 (Zhang et al., 2012; Ishiga et al., 2013; Li et al., 2015). We analyzed the *F. vesca* protein  
391 database and found two ortholog sequences to AtJAZ1 and AtJAZ8, named FvJAZ1 and  
392 FvJAZ8, respectively (Table S1). FvJAZ1/8 proteins contain TIFY and Jas domains; the later  
393 one interacts with COI1 in Arabidopsis (Melotto et al., 2008; Shyu et al., 2012). These domains  
394 were highly conserved between *F. vesca* and other ortholog sequences (Fig. 2A-C). Surprisingly,  
395 we observed that the putative IPMQRK degron sequence in FvJAZ1 was different respect to the  
396 canonical sequence LPIAR(R/K) (Shyu et al. 2012) present in all analyzed JAZ orthologs (Fig.  
397 2C). The JAZ degron is critical because together with COI1 acts as a co-receptor complex,  
398 trapping JA-Ile with high affinity to the COI1 binding pocket (Sheard et al., 2010). On the other  
399 hand, FvJAZ8 contains the same EAR motif sequence (LELRL) than AtJAZ8, which interacts  
400 directly with TOPLESS co-repressor of JA-signaling pathway in a NINJA-independent manner  
401 in Arabidopsis (Shyu et al., 2012). Particularly, neither VvJAZ3, SlJAZ10 and MdJAZ3/4  
402 exhibited LELRL as EAR motif sequence (Fig. 2A). Phylogenetic analysis showed a close



403 relationship between FvJAZ1 and *M. ×domestica* ortholog protein, suggesting a high  
404 conservation of FvJAZ1 orthologs in the Rosaceae family.

405

### 406 **Structural model for FvCOI1**

407

408 Using in silico approaches, we proposed a structural model for FvCOI1 (Fig. 3). First, we tested  
409 its quality using previously validated methodologies (Morales-Quintana et al., 2011; Morales-  
410 Quintana et al., 2012; Galaz et al., 2013), thus we obtained a high-quality structure. The final  
411 structural model for FvCOI1 was used to evaluate COI1 ability to bind two different jasmonate  
412 molecules (JA and JA-Ile) (Fig. 5, 6; and Table 2). We observed that FvCOI1 harbors a surface  
413 pocket, previously described as potential binding site for JA-Ile in AtCOI1 (Sheard et al., 2010).

414

415 The FvCOI1 sequence contained two typical domains, a F-box at the N-terminal region and the  
416 LRR domain at the C-terminal region (Fig. 3), similar to the observed in AtCOI1. The  
417 superposition between AtCOI1 and FvCOI1 structural model showed a high similarity at the F-  
418 box and LRR domains (Fig. S2). Interestingly, FvCOI1 and AtCOI1 did not show integrity at the  
419 LRR domain, because the LRR-8 domain has lost its helix conformation in both structures (Fig.  
420 3B and S2). In contrast, Yan et al. (2009) showed a computational model for the AtCOI1  
421 structure where the LRR-8 is formed by an  $\alpha$ -helix, proposing that the LRR domain integrity is  
422 required for AtCOI1 stability in vivo (Yan et al., 2009). This was observed when authors  
423 evaluated four amino acid substitutions (G369E, G155E, D452A, and L490A) at the LRR  
424 domain, resulting in a reduction of the AtCOI1 stability in vivo. However, none of these  
425 substitutions were in LRR-8 residues. Although, the template and our model do not have an  $\alpha$ -  
426 helix structure in LRR-8, they are stable. It was observed that the obtained trajectory and the  
427 resulting structure after the thermodynamic equilibrations were both stable when the MDS for  
428 FvCOI1 was analyzed. Finally, we noted that LRR-8 is not conserved among the different  
429 analyzed sequences (Fig. 1A) and it was not required for protein-ligand interaction (Fig. 5 and  
430 6).

431

### 432 **FvCOI1-JA-Ile/JA-FvJAZ1/8 complexes formation**

433



434 Using surface plasmon resonance (SPR) technology, Yan et al. (2009) found that AtCOI1, JA-Ile  
435 and AtJAZ1 were sufficient to form a complex, ruling out the possibility that other AtCOI1-  
436 interacting proteins can be involved in JA-Ile perception (Yan et al., 2009). Based on this results,  
437 we modeled the different complexes structures formed by the following components: FvCOI1,  
438 JA-Ile or JA, and FvJAZ1 or FvJAZ8. Thus, we obtained three possibilities for assembling each  
439 protein-ligand-protein complex. Yan et al. (2009) showed that AtCOI1 directly binds to JA-Ile,  
440 and subsequently binds AtJAZ1. Thus, in the present work, we used this previous evidence to set  
441 the temporal order for the conformation of the protein-ligand-protein complex.

442  
443 In Arabidopsis, the Jas domain promotes hormone-dependent interaction between JAZ proteins  
444 and COI1 (Melotto et al., 2008; Chung & Howe, 2009). Structural studies showed that the JAZ1  
445 degron is located at the N-terminal region of the Jas domain, and included five conserved  
446 LPIAR(R/K) residues that sealed JA-Ile in COI1 binding pocket (Sheard et al., 2010). Here, we  
447 showed that FvJAZ1 has a putative degron variant, the IPMQRK sequence (Fig. 2C, S1, S3A).  
448 Despite these differences, the FvJAZ1 showed a favorable HADDOCK score (Table 2), and the  
449 complex formed between FvJAZ1 and FvCOI1-JA-Ile was stable during all MDS (Video S1).  
450 We found that the FvJAZ1 putative degron formed H-bonds with JA-Ile at the C-terminal  
451 (QRK), whereas the N-terminal residues (IPM) interacted directly with FvCOI1, similar to that  
452 found by Sheard et al. (2010) with the AtJAZ1 canonical degron. Similar to FvJAZ1, finger  
453 millet JAZ1 (EcJAZ1) showed a variant sequence respect to the canonical degron (Sen et al.,  
454 2016; Fig. S1). Using an in silico approach, the authors showed that the interaction mode for five  
455 COI1 structural models from monocots was binding to JA-Ile and COR in the presence of  
456 EcJAZ1. The six residues that conform this degron were oriented to 5 Å from the ligand (either  
457 JA-Ile or COR), suggesting a likely interaction with the ligands (Sen et al., 2016). According to  
458 Shyu et al. (2012), alterations within the JAZ degron sequence could lead to a differential  
459 association of JAZ isoforms with COI1 based on JA-Ile levels, in order to activate broad range of  
460 JA responses. In this sense, FvJAZ1 may require a differential JA-Ile accumulation than other  
461 JAZ containing the canonical LPIAR(R/K) degron, to interact with COI1 for promoting FvJAZ1  
462 ubiquitination and subsequently degradation by the 26S proteasome and activation of JA  
463 signaling pathway. Unexpectedly, several (+)-7-*iso*-amino acid conjugates such as (+)-7-*iso*-JA-  
464 Leu, (+)-7-*iso*-JA-Val, (+)-7-*iso*-JA-Ala and (+)-7-*iso*-JA-Met were recently reported as

465 bioactive molecules in Arabidopsis, tomato, rice and tobacco (Yan et al., 2016), which could  
466 bring new ways to regulates JA responses in plants likely via differential interaction strength  
467 between COI1 and JAZ.

468  
469 On the other hand, COI1 has five important residues (R85, R348, Y386, R409 and R496), which  
470 are involved in binding to JA-Ile in Arabidopsis (Sheard et al., 2010). Interestingly, FvCOI1  
471 contained these five conserved residues, but only four are involved in the protein-JA-Ile  
472 interaction, being R406 residue (equivalent to R409 in AtCOI1) not required for the complex  
473 formation. Respects to Arabidopsis JAZ, two adjacent arginine residues located in the degron  
474 motif have a critical role for the interaction with AtCOI1 in the presence of JA-Ile (Melotto et  
475 al., 2008). FvJAZ1 presented a change from R to K residue at the second position (Fig. 2C,  
476 S3A); however the two residues interacted strongly with the FvCOI1 without significant  
477 differences respect to the interaction mode observed for AtCOI1-AtJAZ1. On the contrary,  
478 FvJAZ8 contained M251 and K252 residues at this position (Fig. 2C) and the three first residues  
479 of its degron were different to the corresponding for FvJAZ1. Therefore, FvJAZ8 peptide only  
480 interacts with the FvCOI1-JA-Ile complex through the K residue that is the only one conserved  
481 residue in both FvJAZs degron sequences (Fig. 2C, S3A). As a consequence, the HADDOCK  
482 score was less favorable (Table 2) and the complex was unstable showing a high RMSD value  
483 (Fig. S4). During a long time MDS the interaction was lost (Fig. 6A-C) because FvJAZ8 was  
484 separated from the FvCOI1-JA-Ile complex (Video S2). This evidence is in agreement with  
485 previous results that showed a weaker interaction between AtJAZ8 and AtCOI1 in the presence  
486 of JA-Ile than between AtJAZ1 and AtCOI1 (Shyu et al., 2012).

487  
488 Interestingly, we observed that JA did not leave the FvCOI1 pocket when FvJAZ8 peptide was  
489 present, whereas when FvJAZ1 degron-like peptide was present it did (Fig. 5, 6), supporting the  
490 idea that the presence of the putative degron sequence of FvJAZ1 could be an important feature  
491 for the selection of bioactive JAs, such as JA-Ile in strawberry.

492

## 493 **Conclusions**

494

495 Based on the results presented in this work, we conclude that core components of the early JA  
496 signaling pathway in *F. vesca* such COI1 and JAZ1/8 are highly conserved compared to other  
497 ortholog sequences in plants. Remarkably, FvCOI1 showed a high identity respect to all COI1  
498 orthologs analyzed, while the FvJAZ1/8 exhibited a moderate identity with the ortholog proteins  
499 from Arabidopsis. Particularly, we observed a putative degron sequence (IPMQRK) in FvJAZ1  
500 that is different to the canonical LPIAR(R/K) degron sequence present in non-constitutively  
501 stable JAZ in Arabidopsis. Moreover, we propose that the FvCOI1-JA-Ile-FvJAZ1 complex is  
502 stable, and that the IPMQRK sequence present in FvJAZ1 interacts in a steady manner with  
503 FvCOI1-JA-Ile. Moreover, four amino acid residues observed in the binding site of FvCOI1 are  
504 identical to that observed in AtCOI1.

505  
506 Finally, studying other possibilities on the nature of the interaction temporal order (i.e., FvCOI1-  
507 FvJAZ-JA-Ile and FvJAZ-JA-Ile-FvCOI1) and the use of cofactors to strength the complex  
508 stability will be subjects for future studies.

509

#### 510 **Funding statement**

511

512 This work was supported by the National Commission for Scientific and Technological Research  
513 (CONICYT) of Chile [grants CONICYT, FONDECYT/Regular 1140663 to C.R.F. and  
514 CONICYT PAI/ACADEMIA 79140027 to L.M-Q].

515

#### 516 **Acknowledgements**

517

518 We thank the Center of Bioinformatics and Molecular Simulations (CBSM) at the University of  
519 Talca for providing SCHRÖDINGER suite.

520

#### 521 **References**

522

523 Böttcher C, Burbidge C, di Rienzo V, Boss P, Davies C. 2015. Jasmonic acid-isoleucine  
524 formation in grapevine (*Vitis vinifera* L.) by two enzymes with distinct transcription profiles.  
525 *Journal of Integrative Plant Biology* 57:618-627. DOI: 10.1111/jipb.12321.

526

- 527 Chini A, Gimenez-Ibanez S, Goossens A, Solano R. 2016. Redundancy and specificity in  
528 jasmonate signalling. *Current Opinion in Plant Biology* 33:147-156. DOI:  
529 10.1016/j.pbi.2016.07.005.
- 530
- 531 Chini A, Fonseca S, Fernández G, Adie B, Chico J, Lorenzo O, García-Casado G, López-  
532 Vidriero I, Lozano F, Ponce M, Micol JL, Solano R. 2007. The JAZ family of repressors is the  
533 missing link in jasmonate signalling. *Nature* 448:666-671. DOI: 10.1038/nature06006.
- 534
- 535 Chung HS, Howe GA. 2009. A critical role for the TIFY motif in repression of jasmonate  
536 signaling by a stabilized splice variant of the JASMONATE ZIM-domain protein JAZ10 in  
537 Arabidopsis. *Plant Cell* 21:131–145. DOI: 10.1105/tpc.108.064097.
- 538
- 539 Chung HS, Koo AJ, Gao X, Jayanty S, Thines B, Jones AD, Howe GA. 2008. Regulation and  
540 function of Arabidopsis JASMONATE ZIM-domain genes in response to wounding and  
541 herbivory. *Plant Physiology* 146:952-64. DOI: 10.1104/pp.107.115691.
- 542
- 543 Concha CM, Figueroa NE, Poblete LA, Oñate FA, Schwab W, Figueroa CR. 2013. Methyl  
544 jasmonate treatment induces changes in fruit ripening by modifying the expression of several  
545 ripening genes in *Fragaria chiloensis* fruit. *Plant Physiology and Biochemistry* 70:433-444. DOI:  
546 10.1016/j.plaphy.2013.06.008.
- 547
- 548 de Vries SJ, van Dijk ADJ, Krzeminski M, van Dijk M, Thureau A Hsu, V, Wassenaar T,  
549 Bonvin AMJJ. 2007. HADDOCK versus HADDOCK: new features and performance of  
550 HADDOCK 2.0 on the CAPRI targets. *Proteins: Structure, Function, and Bioinformatics*  
551 69:726–733. DOI: 10.1002/prot.21723.
- 552
- 553 Dominguez C, Boelens R, Bonvin AMJJ. 2003. HADDOCK: a protein–protein docking approach  
554 based on biochemical or biophysical information. *Journal of the American Chemical Society*  
555 125:1731–1737. DOI: 10.1021/ja026939x.
- 556
- 557 Fernández-Calvo P, Chini A, Fernández-Barbero G, Chico J-M, Gimenez-Ibanez S, Geerinck J,  
558 Eeckhout D, Schweizer F, Godoy M, Franco-Zorrilla JM, Pauwels L, Witters E, Puga MI, Paz-  
559 Ares J, Goossens A, Reymond P, De Jaeger G, Solano R. 2011. The Arabidopsis bHLH  
560 transcription factors MYC3 and MYC4 are targets of JAZ repressors and act additively with  
561 MYC2 in the activation of jasmonate responses. *Plant Cell* 23:701–715. DOI:  
562 10.1105/tpc.110.080788.
- 563
- 564 Figueroa P, Browse J. 2015. Male sterility in Arabidopsis induced by overexpression of a  
565 MYC5-SRDX chimeric repressor. *The Plant Journal* 81: 849–860. DOI:10.1111/tpj.12776.
- 566
- 567 Fonseca S, Chini A, Hamberg M, Adie B, Porzel A, Kramell R, Miersch O, Wasternack C,  
568 Solano R. 2009. (+)-7-iso-Jasmonoyl-L-isoleucine is the endogenous bioactive jasmonate.  
569 *Nature Chemical Biology* 5:344-350. DOI: 10.1038/nchembio.161.
- 570

- 571 Galaz S, Morales-Quintana L, Moya-León MA, Herrera R. 2013. Structural analysis of the  
572 alcohol acyltransferase protein family from *Cucumis melo* shows that enzyme activity depends on  
573 an essential solvent channel. *The FEBS Journal* 280:1344–1357. DOI:10.1111/febs.12127.  
574
- 575 Hall TA. 1999. BioEdit: a user-friendly biological sequence alignment editor and analysis  
576 program for Windows 95/98/NT. *Nucleic Acids Symposium Series* 41: 95–98.  
577
- 578 Han GZ. 2016. Evolution of jasmonate biosynthesis and signaling mechanisms. *Journal of*  
579 *Experimental Botany*: erw470. DOI: 10.1093/jxb/erw470.  
580
- 581 Humphrey W, Dalke A, Schulten K. 1996. VMD Visual molecular dynamics. *Journal of*  
582 *Molecular Graphics* 14:33-38. DOI:10.1016/0263-7855(96)00018-5.  
583
- 584 Ishiga Y, Ishiga T, Uppalapati S, Mysore K. 2013. Jasmonate ZIM-Domain (JAZ) protein  
585 regulates host and nonhost pathogen-induced cell death in tomato and *Nicotiana benthamiana*.  
586 *PLoS ONE*: e75728. DOI: 10.1371/journal.pone.0075728.  
587
- 588 Jorgensen WL, Maxwell DS, Tirado-Rives J. 1996. Development and testing of the OPLS all-  
589 atom force field on conformational energetics and properties of organic liquids. *Journal of the*  
590 *American Chemical Society* 118:11225-11236. DOI: 10.1021/ja9621760.  
591
- 592 Katsir L, Schillmiller AL, Staswick PE, He SY, Howe GA. 2008. COI1 is a critical component of  
593 a receptor for jasmonate and the bacterial virulence factor coronatine. *Proceedings of the*  
594 *National Academy of Sciences of the United States of America* 105:7100-7105.  
595 DOI:10.1073/pnas.0802332105.  
596
- 597 Kumar S, Stecher G, Tamura K. 2016. MEGA7: Molecular Evolutionary Genetics Analysis  
598 version 7.0 for bigger datasets. *Molecular Biology and Evolution* 33:1870-1874.  
599 DOI: 10.1093/molbev/msw054.  
600
- 601 Laskowski RA, MacArthur MW, Moss DS, Thornton JM. 1993. PROCHECK: a program to  
602 check the stereochemical quality of protein structures. *Journal of Applied Crystallography*  
603 26:283-291. DOI: 10.1107/S0021889892009944.  
604
- 605 Li X, Yia X, Wang H, Li J, Guo C, Gao H, Zheng Y, Fan C, Wang X. 2015. Genome-wide  
606 identification and analysis of the apple (*Malus x domestica* Borkh.) *TIFY* gene family. *Tree*  
607 *Genetics & Genomics* 11:808. DOI: 10.1007/s11295-014-0808-z.  
608
- 609 Lorenzo O, Chico JM, Sanchez-Serrano JJ, Solano R. 2004. JASMONATE-INSENSITIVE1  
610 encodes a MYC transcription factor essential to discriminate between different jasmonate-  
611 regulated defense responses in *Arabidopsis*. *Plant Cell* 16:1938–1950. DOI: 10.1105/tpc.022319.  
612
- 613 Melotto M, Mecey C, Niu Y, Chung HS, Katsir L, Yao J, Zeng W, Thines B, Staswick P,  
614 Browse J, Howe GA, He SY. 2008. A critical role of two positively charged amino acids in the  
615 Jas motif of *Arabidopsis* JAZ proteins in mediating coronatine- and jasmonoyl isoleucine-

- 616 dependent interactions with the CO11 F-box protein. *The Plant Journal* 55:979–988. DOI:  
617 10.1111/j.1365-313X.2008.03566.x.
- 618
- 619 Morales-Quintana L, Moya-León MA, Herrera R. 2012. Structural analysis of alcohol  
620 acyltransferase from two related climacteric fruit species: potential role of the solvent channel in  
621 substrate selectivity. *Molecular Simulation* 38:912-921. DOI: 10.1080/08927022.2012.672738.
- 622
- 623 Morales-Quintana L, Fuentes L, Gaete-Eastman C, Herrera R, Moya-León MA. 2011. Structural  
624 characterization and substrate specificity of VpAAT1 protein related to ester biosynthesis in  
625 mountain papaya fruit. *Journal of Molecular Graphics and Modelling* 29:635–642. DOI:  
626 10.1016/j.jmgm.2010.11.011.
- 627
- 628 Niu Y, Figueroa P, Browse J. 2011. Characterization of JAZ-interacting bHLH transcription  
629 factors that regulate jasmonate responses in Arabidopsis. *Journal of Experimental Botany*  
630 62:2143-2154. DOI: 10.1093/jxb/erq408.
- 631
- 632 Pauwels L, Barbero GF, Geerinck J, Tilleman S, Grunewald W, Pérez AC, Chico JM, Bossche  
633 RV, Sewell J, Gil E, García-Casado G, Witters E, Inzé D, Long JA, De Jaeger G, Solano R,  
634 Goossens A. 2010. NINJA connects the co-repressor TOPLESS to jasmonate signalling. *Nature*  
635 464:788–791. DOI: 10.1038/nature08854.
- 636
- 637 Perez A, Goossens A. 2013. Jasmonate signalling: a copycat of auxin signalling?. *Plant, Cell &*  
638 *Environment* 36: 2071–2084. DOI:10.1111/pce.12121.
- 639
- 640 Sen S, Kundu S, Dutta S. 2016. Proteomic analysis of JAZ interacting proteins under methyl  
641 jasmonate treatment in finger millet. *Plant Physiology and Biochemistry* 108:79-89. DOI:  
642 10.1016/j.plaphy.2016.05.033.
- 643
- 644 Sheard L, Tan X, Mao H, Withers J, Ben-Nissan G, Hinds T, Kobayashi Y, Hsu F, Sharon M,  
645 Browse J, Yang He S, Rizo J, Howe GA, Zheng N. 2010. Jasmonate perception by inositol-  
646 phosphate-potentiated CO11–JAZ co-receptor. *Nature* 468:400-405. DOI: 10.1038/nature09430.
- 647
- 648 Shen J, Zeng Y, Zhuang X, Sun L, Yao X, Piml P, Jiang L. 2013. Organelle pH in the  
649 Arabidopsis endomembrane system. *Molecular Plant* 5:1419-1437. DOI: 10.1093/mp/sst079.
- 650
- 651 Shyu C, Figueroa P, DePew C, Cooke T, Sheard L, Moreno J, Katsir L, Zheng N, Browse J,  
652 Howe G. 2012. JAZ8 lacks a canonical degron and has an EAR motif that mediates  
653 transcriptional repression of jasmonate responses in Arabidopsis. *Plant Cell* 24:536-550. DOI:  
654 10.1105/tpc.111.093005.
- 655
- 656 Sippl MJ. 1993. Recognition of errors in three-dimensional structures of proteins. *Proteins*  
657 17:355-362. DOI: 10.1002/prot.340170404.
- 658
- 659 Tan X, Calderon-Villalobos L, Sharon M, Zheng C, Robinson C, Estelle M, Zheng N. 2007.  
660 Mechanism of auxin perception by the TIR1 ubiquitin ligase. *Nature* 446:640-645. DOI:  
661 10.1038/nature05731.



- 662  
663 Thines B, Katsir L, Melotto M, Niu Y, Mandaokar A, Liu G, Nomura K, He S, Howe G, Browse  
664 J. 2007. JAZ repressor proteins are targets of the SCF<sup>COI1</sup> complex during jasmonate signalling.  
665 *Nature* 448:661-665. DOI: 10.1038/nature05960.
- 666  
667 Trott O, Olson AJ. 2010. AutoDockVina: improving the speed and accuracy of docking with a  
668 new scoring function, efficient optimization and multithreading. *Journal of Computational*  
669 *Chemistry* 31:455-461. DOI: 10.1002/jcc.21334
- 670  
671 Vanholme B, Grunewald W, Bateman A, Kohchi T, Gheysen G. 2007. The tify family  
672 previously known as ZIM. *Trends in Plant Science* 12:239-244. DOI:  
673 10.1016/j.tplants.2007.04.004.
- 674  
675 Xie D, Feys B, James S, Nieto-Rostro M, Turner J. 1998. COI1: an Arabidopsis gene required  
676 for jasmonate-regulated defense and fertility. *Science* 280:1091-1094. DOI:  
677 10.1126/science.280.5366.1091.
- 678  
679 Xu L, Liu F, Lechner E, Genschik P, Crosby W, Ma H, Peng W, Huang D, Xie D. 2002. The  
680 SCF<sup>COI1</sup> ubiquitin-ligase complexes are required for jasmonate response in Arabidopsis. *Plant*  
681 *Cell* 14:1919-1935. DOI: 10.1105/tpc.003368.
- 682  
683 Yan J, Li S, Gu M, Yao R, Li Y, Chen J, Yang M, Tong J, Xiao L, Nan F, Xie D. 2016.  
684 Endogenous Bioactive Jasmonate Is Composed of a Set of (+)-7- iso- JA-Amino Acid  
685 Conjugates. *Plant Physiology* 172:2154-2164. DOI: 10.1104/pp.16.00906.
- 686  
687 Yan J, Zhang C, Gu M, Bai Z, Zhang W, Qi T, Cheng Z, Peng W, Luo H, Nan F, Wang Z, Xie  
688 D. 2009. The Arabidopsis CORONATINE INSENSITIVE1 Protein Is a Jasmonate Receptor.  
689 *Plant Cell* 21:2220-2236. DOI: 10.1105/tpc.109.065730.
- 690  
691 Yan Y, Stolz S, Chetelat A, Reymond P, Pagni M, Dubugnon L, Farmer EE. 2007. A  
692 downstream mediator in the growth repression limb of the jasmonate pathway. *Plant Cell*  
693 19:2470-2483. DOI: 10.1105/tpc.107.050708.
- 694  
695 Zhang Y, Gao M, Singer S, Fei Z, Wang H, Wang X. 2012. Genome-wide identification and  
696 analysis of the TIFY gene family in grape. *PLoS ONE*: e44465. DOI:  
697 10.1371/journal.pone.0044465.

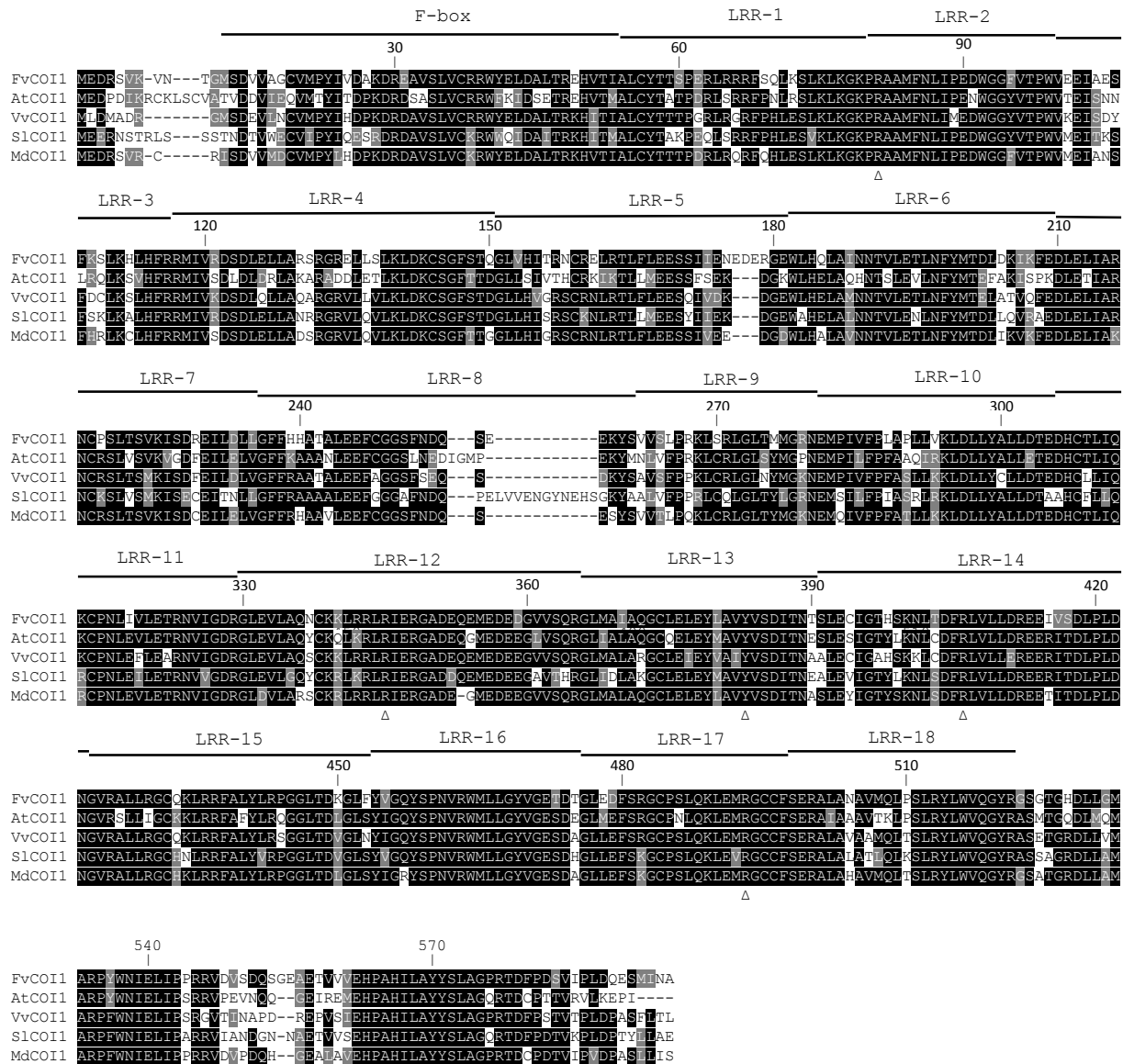


698 **Figure 1**

699

700

701

**A**

702

703

704

705

706

707

708

709

710

711 **Fig. 1 (continued)**

712

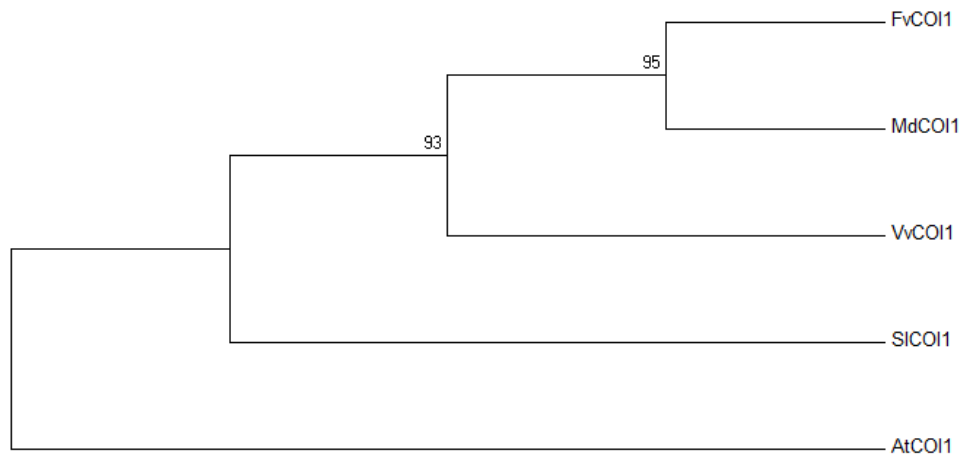
713

714

715

716

**B**



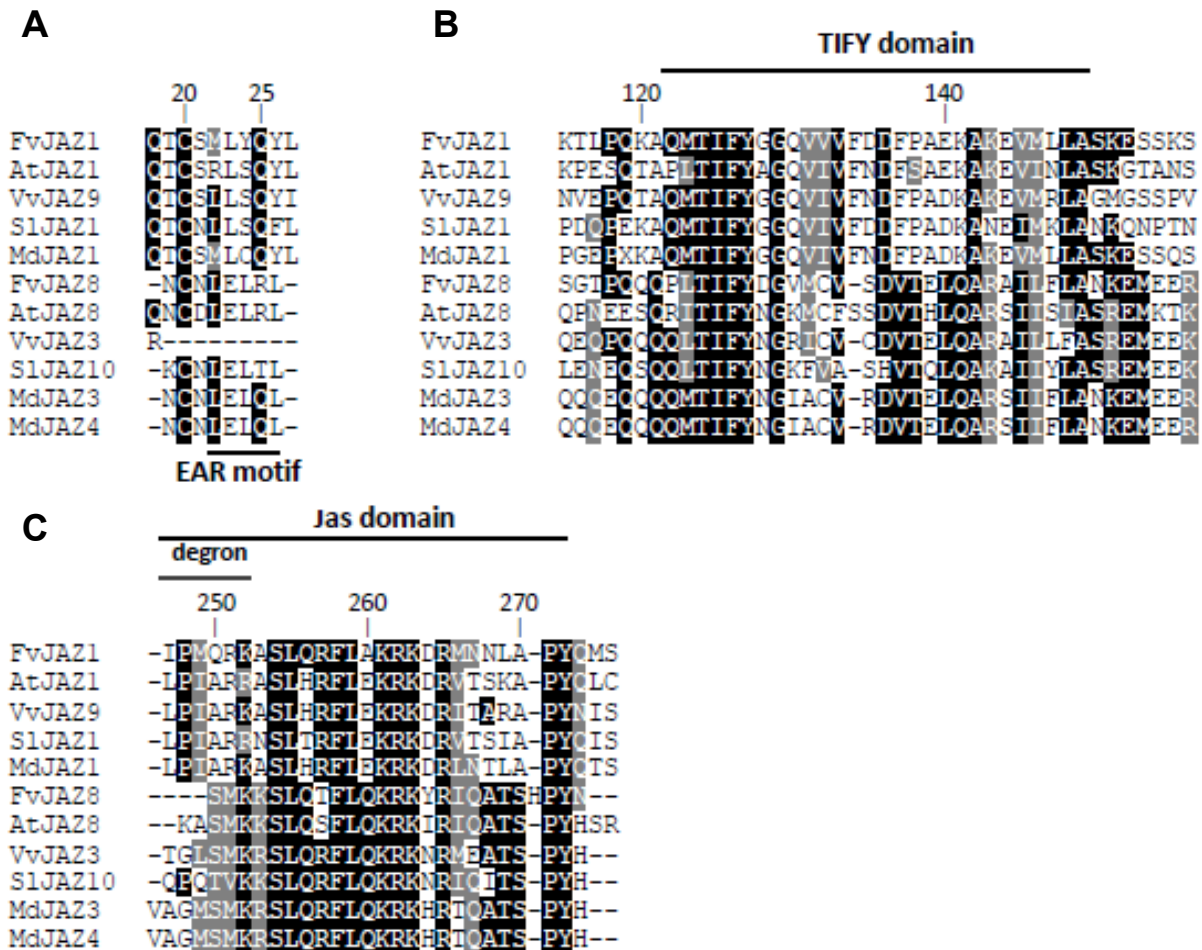
717

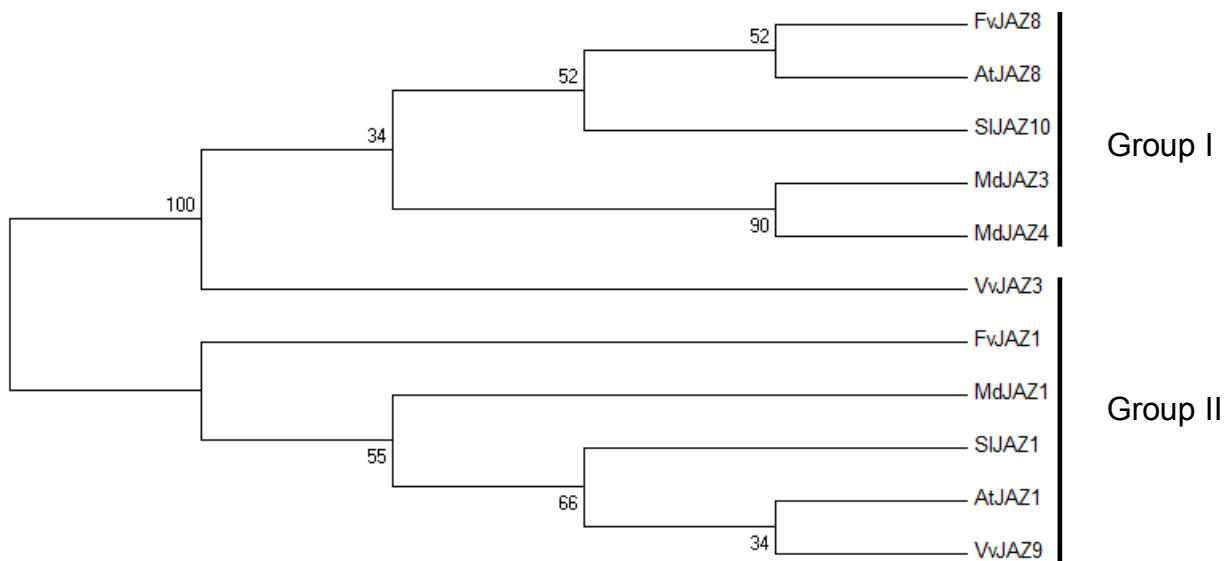
718

719

720

721 **Figure 1. Comparison of FvCOI1 with ortholog proteins.** (A) Alignment of the inferred  
 722 amino acid sequences of FvCOI1 with other orthologs. Gaps are indicated by dashes, letters with  
 723 black background represent identical amino acid residues, and letters with grey background  
 724 represent similar residues. Open triangles ( $\Delta$ ) indicate conserved residues for JA-Ile binding in  
 725 COI1. F-box and the 18 LRR domains are shown. (B) Phylogenetic analysis of FvCOI1 sequence  
 726 with other orthologs. For GenBank accession numbers see Material and Methods section.  
 727 FvCOI1, *Fragaria vesca* COI1; AtCOI1, *Arabidopsis thaliana* COI1; VvCOI1, *Vitis vinifera*  
 728 COI1; SiCOI1, *Solanum lycopersicum* COI1; and MdCOI1, *Malus domestica* COI1. F-box: F-  
 729 box domain, LRR: leucine-rich repeat domain.

730 **Figure 2**731  
732  
733734  
735  
736  
737  
738  
739  
740  
741  
742  
743  
744  
745  
746  
747  
748  
749

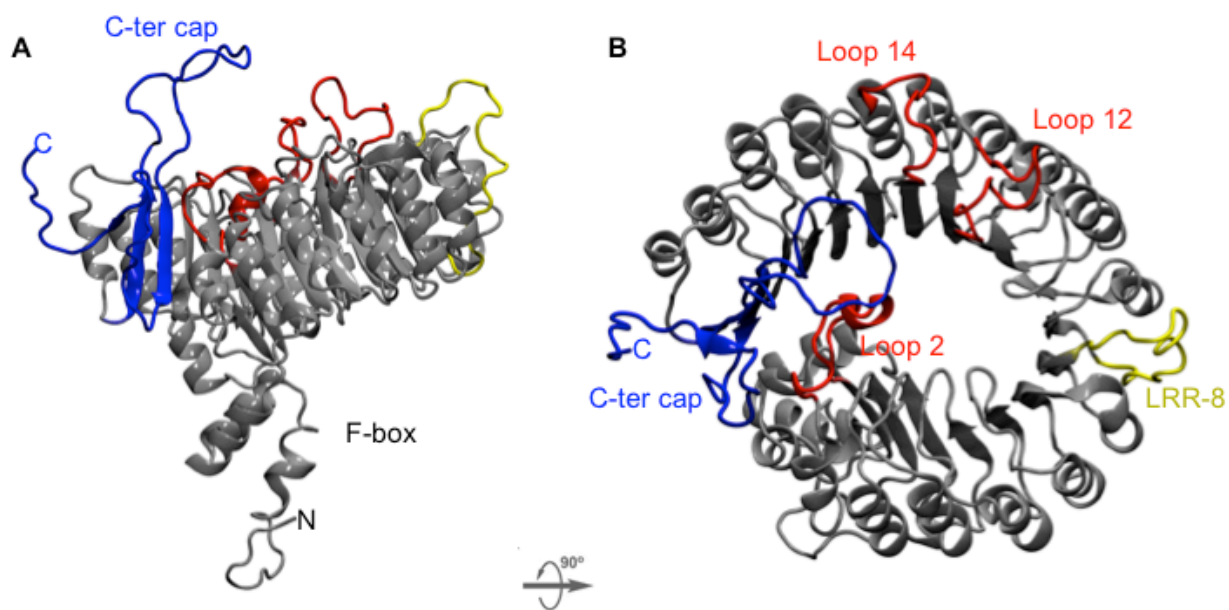
750 **Fig. 2 (continued)**751  
752  
753  
754  
755  
756  
757  
758  
759  
760  
761  
762  
763  
764  
765  
766  
767  
768  
769  
770  
771  
772  
773  
774  
775**D**

776 **Figure 2. Comparison of main domains and motifs of FvJAZ1/8 with ortholog sequences.**  
 777 (A), (B) and (C) Alignments of the inferred full-length amino acid sequences of EAR motif,  
 778 TIFY and Jas domains of FvJAZ1 and FvJAZ8 with their orthologs, respectively. The degron  
 779 sequences are shown within the Jas domain. Gaps are indicated by dashes, letters with black  
 780 background represent identical amino acid residues, and letters with grey background represent  
 781 similar amino acid residues. (B) Phylogenetic analysis of FvJAZ1/8 amino acid sequence with  
 782 orthologs ones. Group I and group II include orthologs for FvJAZ8 and FvJAZ1, respectively.  
 783 For GenBank accession numbers see Material and Methods section. FvJAZ1/8, *Fragaria vesca*  
 784 JAZ1/8; AtJAZ1/8, *Arabidopsis thaliana* JAZ1/8; VvJAZ9/3, *Vitis vinifera* JAZ9/3; SIJAZ1/10,  
 785 *Solanum lycopersicum* JAZ1/10; and MdJAZ1/3/4, *Malus ×domestica* JAZ1/3/4.

786 **Figure 3**

787

788



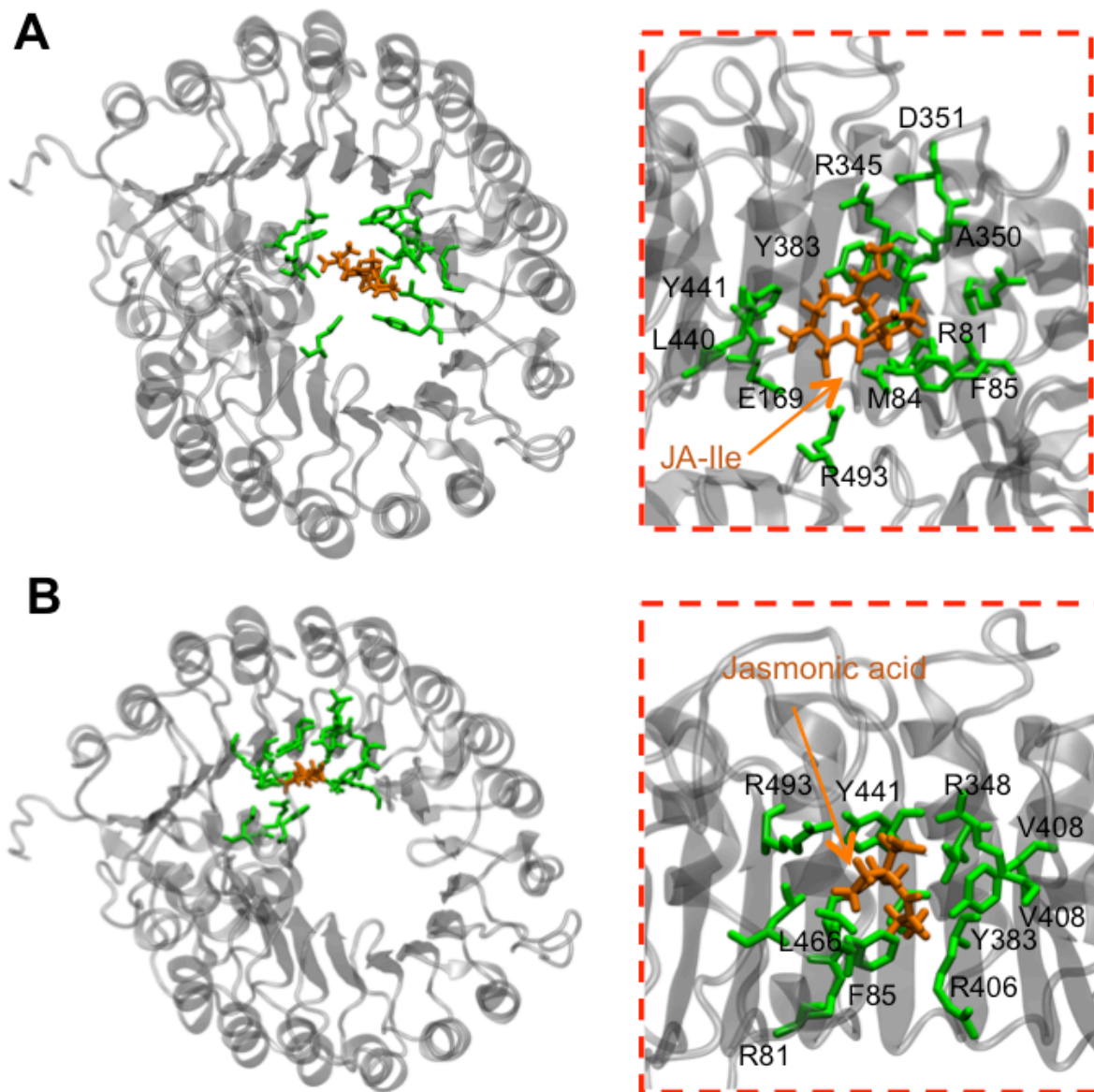
789

790

791

792 **Figure 3. Structural model for COI1.** Two views of the FvCOI1 structural model are shown as  
793 NewCartoon representation (A and B). The F-box and LRR domains of FvCOI1 are shown in  
794 gray color. The C-terminal cap is shown in blue while the three important loops forming the  
795 hormone pocket in FvCOI1 are shown in red. The LRR-8 domain is represented in yellow.

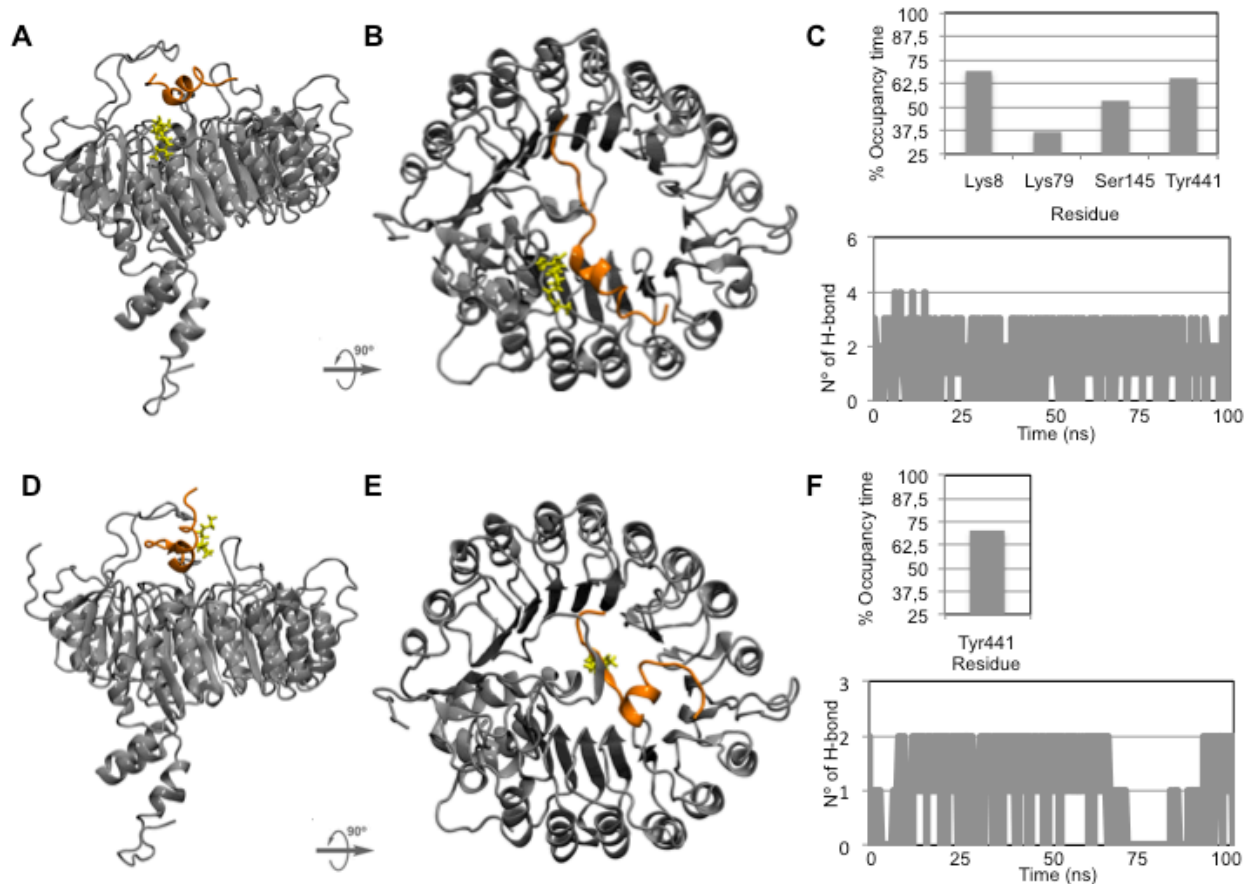
796 **Figure 4**  
 797  
 798



799  
 800  
 801 **Figure 4. Ligand binding analysis based on a refined FvCOI1 model.** A detailed view of the  
 802 hormone-binding pocket site of FvCOI1 showing the residues involved in the interaction  
 803 (represented in green) with JA-Ile (A), and jasmonic acid (B) (represented in orange).  
 804 Magnifications of the hormone binding pockets are shown at the right side.



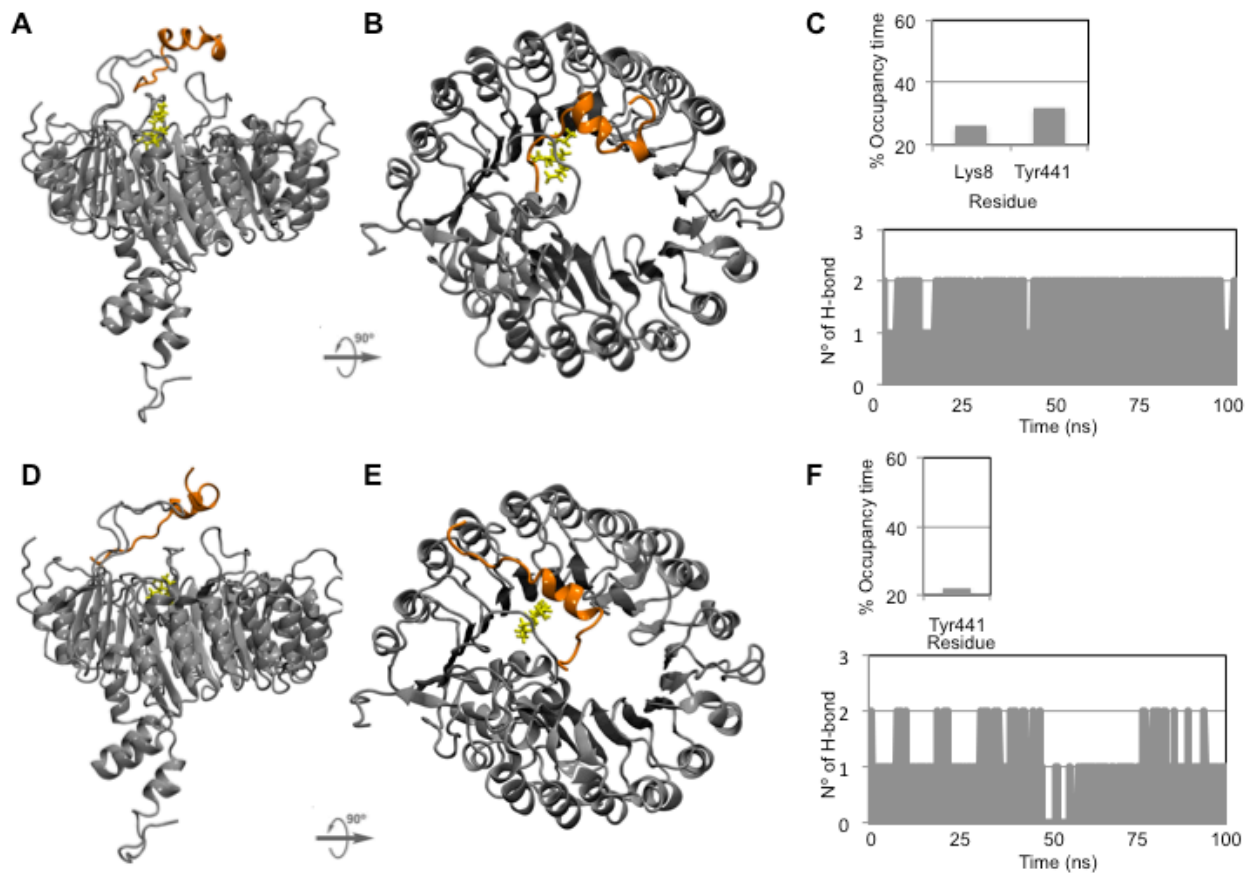
805 **Figure 5**  
 806  
 807



808  
 809  
 810  
 811 **Figure 5. MDS analyses of the interactions in FvCOI1-JA-Ile-FvJAZ1 (A, B, C) and**  
 812 **FvCOI1-JA-FvJAZ1 complexes (D, E, F).** A frontal (A) and top (B) views of interaction  
 813 between the FvCOI1-JA-Ile complex and FvJAZ1. (C) Top graph shows the time percentage that  
 814 a hydrogen bond between a particular amino acid residue of FvCOI1 and the JA-Ile or FvJAZ1 is  
 815 established. Only values greater than or equal to 30% frequency are shown in the graph. Lower  
 816 graph shows the number of total H-bonds formed by the complex. A frontal (D) and top (E)  
 817 views of the interaction between the FvCOI1-JA complex and FvJAZ1. (C) Top graph shows the  
 818 time percentage that hydrogen bonds between Y441 of FvCOI1 and the JA or FvJAZ1 is  
 819 established. Lower graph shows the number of total H-bonds formed by the complex.



820 **Figure 6**  
 821  
 822



823  
 824  
 825  
 826 **Figure 6. MDS analyses of the interactions in FvCOI1-JA-Ile-FvJAZ8 (A, B, C) and**  
 827 **FvCOI1-JA-FvJAZ8 complexes (D, E, F).** A frontal (A) and top (B) views of interaction  
 828 between the FvCOI1-JA-Ile complex and FvJAZ8. (C) Top graph shows the time percentage that  
 829 a hydrogen bond between a particular amino acid residue of FvCOI1 and the JA-Ile or FvJAZ1 is  
 830 established. Only values greater than or equal to 30% frequency are shown in the graph. Lower  
 831 graph shows the number of total H-bonds formed by the complex. A frontal (D) and top (E)  
 832 views of the interaction between the FvCOI1-JA complex and FvJAZ8. (C) Top graph shows the  
 833 time percentage that hydrogen bonds between Y441 of FvCOI1 and the JA or FvJAZ8 is  
 834 established. Lower graph shows the number of total H-bonds formed by the complex.

835 **Tables**

836

837 **Table 1. Affinity energy for the interaction between FvCOI1 protein and JA or JA-Ile**  
838 **ligands**

839

840

Ligands	FvCOI1
	Affinity energy (kcal mol <sup>-1</sup> )
Jasmonic acid (JA)	-1.3 <sup>a</sup> ± 0.2
(+)-7- <i>iso</i> -jasmonoyl-isoleucine (JA-Ile)	-11.1 <sup>b</sup> ± 0.2

841

842 Data correspond to the mean ± SE for the best protein-ligand conformation of five independent docking  
843 runs for each ligand. Different lower-case letters indicate significant differences between each ligand  
844 (Tukey HSD test,  $p \leq 0.05$ ).

845

846 **Table 2. HADDOCK score obtained for the interaction between FvJAZ1 and FvJAZ8 with**  
847 **FvCOI1-ligand complexes**

848  
849

Protein	HADDOCK score	
	FvCOI1-JA-Ile	FvCOI1-JA
FvJAZ1	-71.3 <sup>a</sup> ± 14.7	-43.3 <sup>b</sup> ± 5.3
FvJAZ8	-37.1 <sup>a</sup> ± 3.3	-30.3 <sup>a</sup> ± 8.4

850  
851 Data correspond to the mean ± SE for the best protein-ligand-protein conformation of three independent  
852 docking runs for each ligand. Different lower-case letters indicate significant differences between each  
853 FvJAZ protein with the FvCOI1-ligand complex (Tukey HSD test,  $p \leq 0.05$ ).